ADVANCED FUNCTIONAL MATERIALS
www.afm-journal.de

Solution-Tube-Based Volume Effect Triboelectric Nanogenerator with Salt and pH Sensitivity

Qitao Zhou, Boyou Wang, Along Gao, Wenxia Xu, Kang Zhou, Jing Pan, Guowen Meng, Caofeng Pan,* and Fan Xia**

Due to the advantages of natural softness and flexibility of water, liquid–solid-based triboelectric nanogenerators (TENGs) have aroused wide attention recently and much effort has been devoted to improving its output performance. Herein, the performance of liquid–solid-based TENG is greatly improved through two simple steps. First, an end electrode is added into the traditional tube-based TENG and the volume effect is successfully realized, with the output voltage improved by ≈40 times to 240 V. Then, the output voltage of the tube-based TENG can be further improved to 461 V by replacing water with NaOH solution and an impressive peak power density of 1910 Wm^{-3} and an average power density of 459 Wm^{-3} can be achieved. Additionally, the demonstration shows that the solution-tube-based volume effect TENG can work well at various operation modes and generate power from multiple mechanical energy sources. In addition to wearable human motion energy recovery, wave energy recovery, and electrochemical cathodic protection systems, the device also shows its application potential in biochemical sensing based on the solute concentration-dependent output signal.

1. Introduction

With the aggravation of energy crisis and environmental problems, clean and sustainable energy harvesting devices capable of extracting electrical energy from ambient environments, such as mechanical vibrations, heat and light has been extensively investigated during the last decade. The emerging novel power generation technology of triboelectric nanogenerator (TENG) is attracting increasing attention due to its wide application prospect. From small wearable portable energy devices to the blue energy harvesting network facing the ocean, TENGs have shown great potential.[1–3] However, the conventional solid-solid-based TENG devices often face a difficult problem to balance. On the one hand, in order to obtain high output, the intimacy contact and sufficient interaction between the two tribo-materials should be realized. But the sufficient interaction would simultaneously aggravate the abrasion and consumption of the friction materials. To solve this problem, various strategies have been proposed, such as using soft contacted structure/materials to enhance the effective contact area,[4–6] employing the non-contact mode to reduce the abrasion of material,[7] or utilizing a boundary lubrication film.[8]

In addition to the solutions mentioned above, TENGs based on solid-liquid interface can also resolve these problems. Water, with its natural softness and flexibility can contact the solid surface intimately and barely abrade solid surfaces. Besides, the TENG based on solid-liquid interface has an inherent advantage of humidity resistance.[9] Unfortunately, for a long time, most solid-liquid TENGs typically consist of a hydrophobic electret polymer layer for creating contact electrification with water and a metal electrode for charge collection. However due to the single-electrode design, they can only utilize half of the triboelectric charges and thus exhibited limited energy conversion efficiency.[10] Recently Wang et al. demonstrated a droplet-based electricity generator with double-electrode architecture. This device architecture allows for the formation of a closed-loop circuit when an impinged water droplet on top polytetrafluoroethylene (PTFE) surface spreads to the aluminum electrodes, resulting in a extremely high power density.[11,12] As the spreading of the droplet bridges the disconnected components into a closed-looped, electrical system and transforms the conventional interfacial effect into the desirable so-called ‘volume effect’. However, at present, TENGs based on volume effect mainly focus on recovering the mechanical energy of flowing water droplets or water columns.[13–15] Thus, the water here is a

Q. Zhou, B. Wang, A. Gao, W. Xu, K. Zhou, J. Pan, F. Xia
State Key Laboratory of Biogeology and Environmental Geology
Engineering Research Center of Nano-Geomaterials of the Ministry of Education
Faculty of Materials Science and Chemistry
China University of Geosciences
Wuhan 430074, China
E-mail: xiafan@cug.edu.cn
G. Meng
Key Laboratory of Materials Physics
and Anhui Key Laboratory of Nanomaterials and Nanotechnology
Institute of Solid State Physics
HFIPS
Chinese Academy of Sciences
Hefei 230031, China
E-mail: gwmeng@issp.ac.cn
C. Pan
Beijing Institute of Nanoenergy and Nanosystems
Chinese Academy of Sciences
Beijing 100083, China
E-mail: cfpan@binn.cas.cn

The ORCID identification number(s) for the author(s) of this article can be found under https://doi.org/10.1002/adfm.202209100.

DOI: 10.1002/adfm.202209100

disposable friction material, which cannot be reused directly. As a result, their application fields are limited. On the other hand, in tube-based solid-liquid TENGs, water can be used as a reusable friction material to give better play to its advantages by sealing water in a confined space.[16,17] However, the performances of tube-based solid-liquid TENGs need to be further improved.

In this work, the volume effect is successfully integrated into the tube-based TENG, which improves the output performance by two orders of magnitude compared with ordinary single electrode device. Moreover, by adding a certain concentration of alkaline solution, the performance of the device is further improved. At the same time, the effects of a series of salt or acidic solutions on the performance of the device are also discussed. Furthermore, the applications of the device in wearable mechanical energy recovery device, wave energy harvesting and electrochemical cathodic protection system are demonstrated.

2. Results and Discussion

Figure 1a illustrates the device configuration of the solution-tube-based volume effect triboelectric nanogenerator (STVE-TENG). A PTFE tube (with the length of 10 cm and outer diameter of 1.8 cm) was utilized as a negative tribo-material and the container of the water or solution. DI water or solution containing different solutes was filled into the PTFE tube as the positive tribo-material. The two ends of the tube were sealed by PTFE cover. A circle of Cu wire was arranged at the bottom of one cover and led out through a small hole as one of the electrodes. A Cu tape was wrapped in the middle of the outer surface of the tube as another electrode. Figure 1b shows the photo of the device. Figure 1c shows potential applications of the device, such as self-powered buoy system, wearable self-powered device, TENG networks for harvesting large-scale blue energy or self-powered electrochemical cathodic protection system.

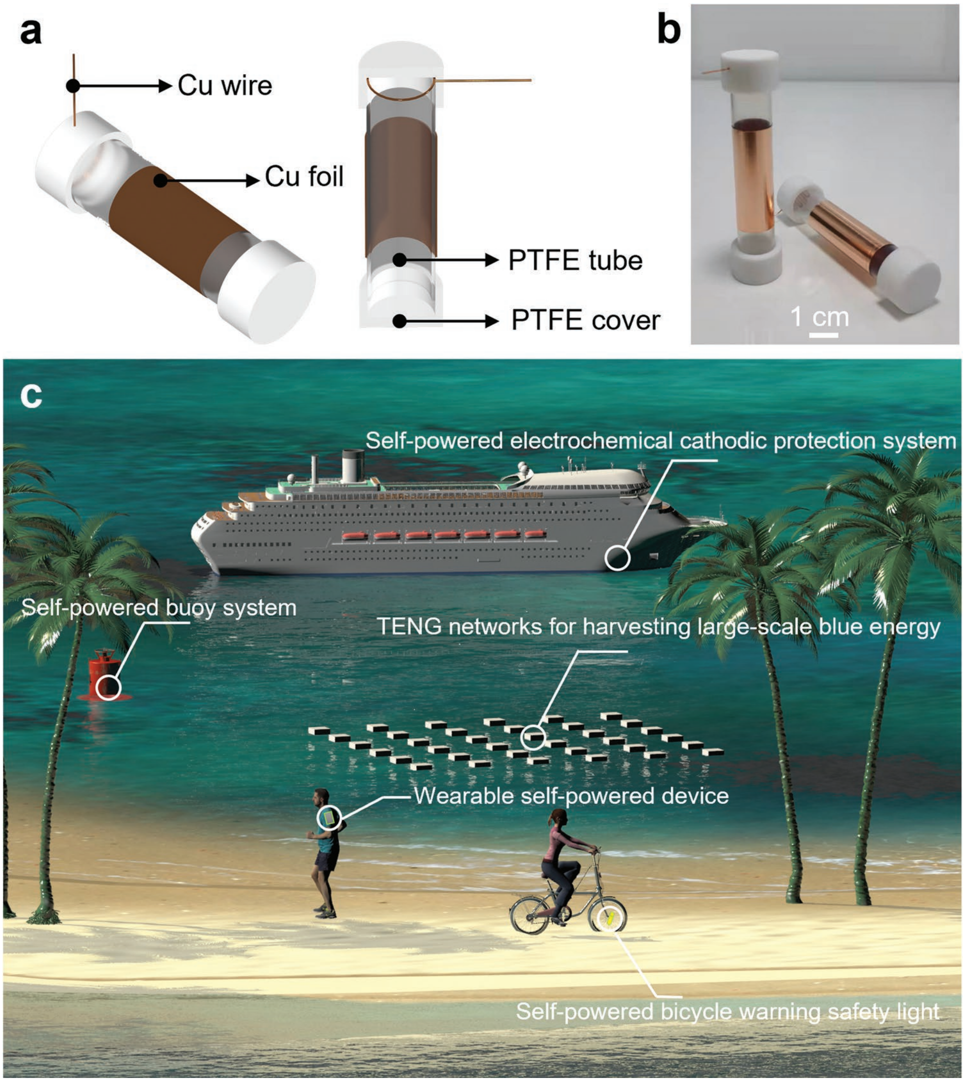

Figure 1. The structure of the STVE-TENG and its potential application scenarios. a) Schematics of the STVE-TENGs. b) Photograph of the STVE-TENGs. c) Application potential of the STVE-TENG in wearable or wave energy collection and electrochemical cathodic protection system.

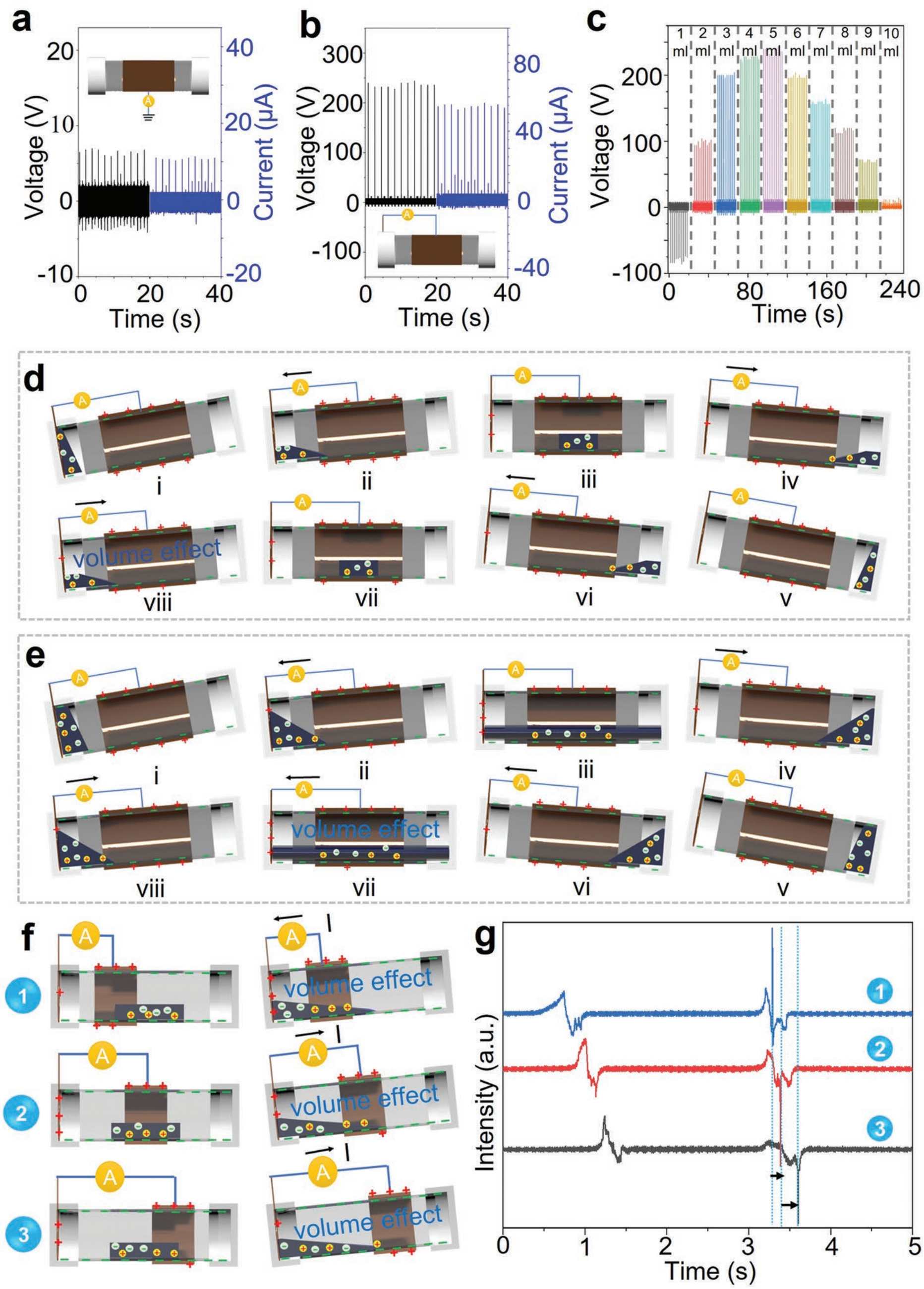

Figure 2. Electrical output characteristics and the working principles of the STVE-TENGs. a) The output performance of the tube-based TENG without end electrode. b) The output performance of the STVE-TENG. c) The output voltages of the STVE-TENGs as a function of the volume of water added. d,e) The working principles of the STVE-TENGs when 1 and 5 mL water are added respectively. f,g) Characteristics of output voltage signals of the STVE-TENGs with 2 cm wide Cu foil electrode when adjusting the spacing between Cu foil electrode and end electrode.

By comparing the performance of devices with and without end electrodes as shown in **Figure 2**a,b, the importance of introducing volume effect to improve the output performance of the device is reflected. It can be seen that the output voltage of the device without end electrode is 7 V, and the output voltage of the device increases to 240 V after adding end electrode (Video S1, Supporting Information). The corresponding short-circuit current also increases from 11 μA increased to 56 μA. The improvement of performance proves that the volume effect has been successfully applied in our device. Then to optimize the system performance, a series of devices with different geometric parameters were fabricated. First, the width of Cu foil has been adjusted. From Figure S1 (Supporting Information), it can be seen that the outputs of STVE-TENG are positively proportional to the width as well as the area of the electrodes. Using a STVE-TENG unit with the tube diameter of 1.8 cm and Cu foil electrode width of 5 cm, outputs of 240 V were achieved. Then the volume of water in the device is discussed as another parameter. It can be seen that, when the volume of water changes from 1 to 8 mL, the characteristics of the output electrical signal show a significant change (Figure 2c). Through experiments, we found that the main reason for this result is that the working mechanism of the device is different when there is only 1 mL water.

Figure 2d,e describe the working principle of the device under two different conditions. According to the triboelectric series, water is much more positive than PTFE. Thus, after the device starts to operate, the PTFE surface will soon be negatively charged under the interaction of water flow and PTFE surface. When 1 mL water is filled, due to its small volume, only a small part of the device can be covered in the flow process (Figure 2d). Then, as shown in Figure 2d(i,ii), when water flows from the end electrode side to the other side, a potential difference is formed between the Cu foil electrode and the end electrode due to the neutralization of the positive charge in the water to the negative charge on the corresponding PTFE surface above the Cu foil. Accordingly, electrons flow from the end electrode to the Cu foil electrode. As the water continues to flow (Figure 2d(iii,iv)), the neutralization disappears, so the device generates a reverse current. Next, as shown in Figure 2d(v,vi), when 1 mL water flows toward the end electrode side, due to its small size, it is unable to contact the end electrode immediately. Therefore, as mentioned above, the potential difference caused by the neutralization phenomenon will produce a current. Then the water continues to flow and contacts the end electrode, triggering the volume effect, so a strong output signal can be obtained (Figure 2d(viii)). When the volume of water changes from 2 to 5 mL, the basic working principle is similar. The difference is that due to the larger volume of water, only a small tilt amplitude can trigger the volume effect (Figure 2e(vi,vii)). Therefore, compared with Figure 2d, the time of triggering the volume effect is advanced, resulting in the opposite direction of the high voltage output signal.

In order to prove that this sharp signal peak is caused by the instant of contact between water and end electrode, we did the following experiments. As shown in Figure 2f, when the width of the Cu foil electrode is reduced and the position of the Cu foil on the PTFE tube is moved at the same time, the corresponding time point of contact between water and the end electrode can be adjusted. It should be noted that the positive probe of the oscilloscope is connected to the Cu foil electrode and the negative probe is connected to the end electrode in the experiment. Therefore, as the liquid flows closer to the Cu foil electrode and farther away from the Cu foil electrode, a relatively slow changing positive signal and a negative signal can be obtained respectively, which is similar to the device in the single electrode mode. Moreover, at this time, the volume of water in the tube is 1 mL. Due to the hydrophobic property of PTFE, when the tube is laid flat, the water column is distributed in the middle of the tube and there is no contact with both ends.

Thus, in case 1, as the right end of the tube rises, the liquid has contacted the end electrode while flowing to the Cu foil electrode and completely covering it. Therefore, with the inherently slow changing positive signal, there is a sharp positive signal due to the volume effect being triggered. It can be simply understood that in this case, the volume effect helps electrons flow from the end electrode to the Cu foil electrode. In case 3, since the distance between the Cu foil electrode and the end electrode is very long, only a part of the Cu foil electrode is covered by the solution when it is laid flat. When the right end of the tube rises, the solution moves away from the Cu foil electrode. Then, when only a small part of the Cu foil electrode is covered by the liquid, the liquid contacts the end electrode and triggers the volume effect. Therefore, there is a sharp negative signal at the end of the inherently slow changing negative signal. Correspondingly, it can be simply considered that the volume effect helps electrons flow from the Cu foil electrode to the end electrode. Accordingly, since the position of the Cu foil electrode in case 2 is between the above two cases, the position where the sharp negative signal occurs is also between the above two cases. These results show that the sharp output peak is indeed caused by the volume effect triggered by the contact of water with the end electrode. Meanwhile, the working mechanism we hypothesized is also reasonable.

The above results have proved that the performance of STVE-TENG has been greatly improved by introducing volume effect. Then, the performance of STVE-TENG was further modulated by adjusting the salt concentration or pH value (**Figure 3**). First, to evaluate the response of the STVE-TENG to different pH of solution, we tested the devices containing different acid or alkali concentrations. The electrolyte was obtained by dissolving NaOH and KOH or diluting high concentration HCl into water. First, when an alkaline solution was used, as more hydroxyl ions were provided and enhanced the charge density at the PTFE surface, the output voltage increased from 300 to 461 V when the concentration of NaOH was elevated from 0.1 to 1 mM (Video S2, Supporting Information). This is because, it is known that fluoropolymer materials tend to absorb negative charges, i.e., hydroxyl ions, from water, which significantly contributes to the charge storage and therefore plays an essential role in the output characteristics of liquid–solid TENGs.[18–20] At the same time, it is remarkable that when the concentration of NaOH solution in the device is 1 mM, the short-circuit current of the device reaches ≈880 μA (Figure S2, Supporting Information). However, when the concentration of NaOH was further increased from 2 to 100 mM, the output voltage dropped again, and this is likely due to the excessive number of negative ions hindering the reservation of positive charges on the droplet surface during the friction.[10,21] When NaOH solution is replaced by KOH solution, it also shows a similar trend (Figure S3, Supporting Information). Since the Cu wire electrode will be in direct contact with the solution, we also tested the stability of the device. From Figure S4 (Supporting Information), it can be seen that for NaOH solution, the performance of the device is basically stable during 24 h. of continuous operation. In addition, the device has similar high output voltage and excellent stability after replacing Cu wire electrode with Ni wire electrode. However, when Al wire is selected as the top electrode, the output performance of the device shows a continuous downward trend. This is because Al reacts with NaOH solution to change the composition of the solution.

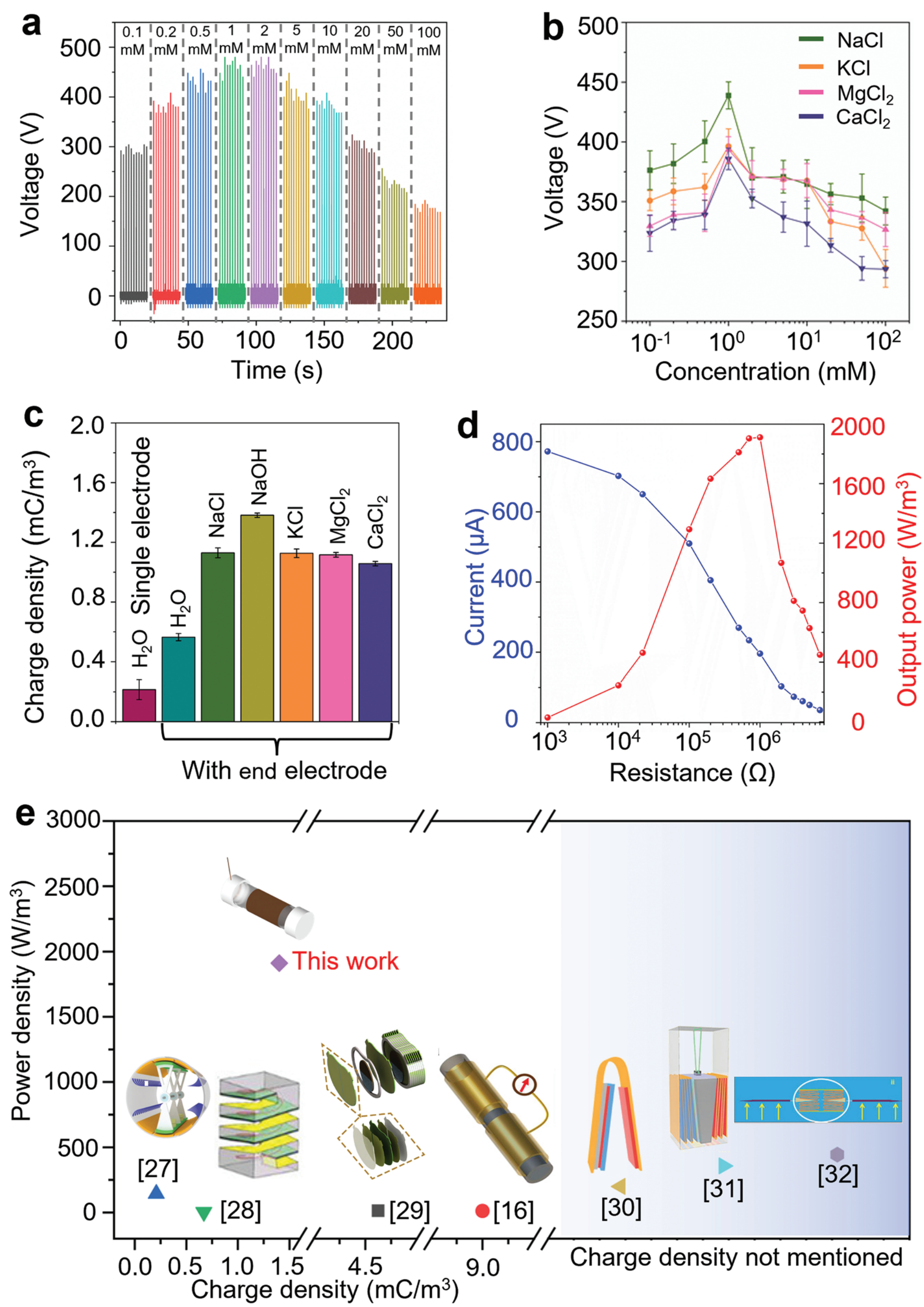

Figure 3. Output performance of the STVE-TENGs after adding different salt solutions or alkaline solutions. a) Output voltages of the STVE-TENG, as a function of NaOH concentration. b) Output voltages of the STVE-TENG, a function of different concentrations of different salts. c) Charge density generated from different types of tube-based TENGs with different solution. d) Evolution of current peak and power peak with the increase of external resistance for the STVE-TENGs with 5 mL of 1 mM NaOH solution. e) Comparison of the peak power density and charge density value obtained in this work with other reports.[16,27–32] (Reference information: Reproduced with permission.[27] Copyright 2020, John Wiley & Sons. Reproduced with permission.[28] Copyright 2018, John Wiley & Sons. Reproduced with permission.[29] Copyright 2019, Elsevier. Reproduced with permission.[16] Copyright 2021, John Wiley & Sons. Reproduced with permission.[30] Copyright 2021, John Wiley & Sons. Reproduced with permission.[31] Copyright 2022, John Wiley & Sons. Reproduced with permission.[32] Copyright 2020, John Wiley & Sons.)

Then, we found that as the concentration of HCl in the solution increases from 0.1 mM to 5 M, the output voltage decreased monotonically from 360 to 2 V (Figure S5, Supporting Information). Low concentration HCl showed better performance than DI water because it increases the conductivity of the solution.[20] At the same time, due to the concentration of hydroxyl ions is largely reduced in the acidic solution as compared to DI water, the density of the trapped negative charges at the PTFE surface is reduced accordingly. Therefore, its output performance was weaker than that of device containing NaOH solution, and decreased faster with the increase of HCl concentration. When the concentration of HCl increased to 10 м, the polarity of triboelectricity reversed (−22 V). This is due to the relative excess of hydrogen ions in the solution, and a large amount of hydrogen ions are adsorbed on the surface of PTFE. The effect can be seen as the formation of a new positively charged surface. The corresponding transferred charge of devices containing HCl solutions with low (0.1 mм) or high (10 м) concentration also confirms above results (Figure S6, Supporting Information).

Other salt solutions, including $MgCl_2$, $CaCl_2$, NaCl, and KCl solutions, are also measured here. As shown in Figure 3b and Figure S7 (Supporting Information), the output of STVE-TENG based on these kinds of solutions is similar to that of STVE-TENG based on NaOH solution, they all showed a trend of first increasing and then decreasing. In the low concentration range, the output voltage shows a gradual upward trend. One possible explanation is that within a certain concentration range, the salt solution with a certain conductivity will promote the conversion between the built-in electric field of the interface, because the low concentration of salt concentration will behave more like a conductor with the increase of the conductivity.[22] Therefore, electrons will be more easily transferred from the sliding surface of water to another. As the previous study indicated that the introduction of ions will cause the inhibitory effect of electron transfer, so there will be competition between ions and electrons.[23] Due to the possible competitive effect of electron transfer and ion absorption with ion concentration changes in this process, and finally shows the variation law of output performance on ion concentration.[24] The above result show that the performance of our devices can also be improved by simply adding a salt solution similar to seawater without environmental pollution. At the same time, because the performance of STVE-TENG changes with the change of concentration of salt or acid/base in the solution, which shows its application potential in the field of biochemical sensors.[25,26] Due to its relatively low selectivity, it is still mainly limited to concentration sensing. The corresponding transferred charge of devices containing different solutions also shows similar trends (Figure S8, Supporting Information).

By varying the external load of the circuit, the output characteristics of the STVE-TENG were obtained and the output power (P) was calculated through the following equations

$$P_{\mathrm{peak}} = I_{\mathrm{peak}}^2 R \tag{1}$$

$$P_{\mathrm{ave}} = \frac{\int_0^T I^2 R dt}{T} \tag{2}$$

where I_{peak} is the peak value of the current amplitude, R is the resistance of the external load, T is the period of the output and I is the output current. For our devices, the maximum output power of 38.4 mW was achieved when the external resistance was 1 MΩ (Figure 3e). Since the volume of the device is ≈20.1 cm^3, the peak power density was calculated to be 1910 Wm^{-3} and the average power density was calculated to be 459 Wm^{-3}. On the other hand, the volumetric charge density was calculated to be 1.38 mC m^{-3}. Compared with the existing devices, it can be seen that although our device does not have the highest volumetric charge density, it has the highest peak power density at present.[16,27–32] In contrast, the peak power density of the corresponding single electrode device is only 2.43 Wm^{-3} (Figure S9, Supporting Information) and the average power density was calculated to be 0.4 Wm^{-3}. Meanwhile, the peak power density of the STVE-TENG with DI water is ≈232 Wm^{-3} (Figure S10, Supporting Information) and the average power density was calculated to be 49 Wm^{-3}. The above results show that the output performance is greatly improved after the volume effect is introduced.

The STVE-TENG enabled us to develop a self-powered safety system and to power LEDs. As can be seen from **Figure 4**a,b, the system can be worn on the body or installed on a bicycle. When worn on the arm, 24 LEDs can be lit by swinging the arm (Video S3, Supporting Information). This shows its potential as a wearable power supply for some biochemical sensors.[33,34] Similarly, as the bicycle wheel rotates, the solution flows back and forth in the device, and the generated electric energy can light up 50 LEDs (Video S4, Supporting Information). The safety protection function is realized by recycling the moving mechanical energy and lighting the LEDs. The electric energy generated by running three devices at the same time can light up 150 LEDs (Video S5, Supporting Information). To demonstrate the functionality of the STVE-TENG in practical scenarios, we placed 15 STVE-TENG units into a sealed box for energy harvesting from water waves. However, in the real environment, for example, the fluctuation direction of waves is random. In order to ensure the output performance, the STVE-TENG units were arranged in different directions. The paralleled STVE-TENG units were connected with a bridge rectifier to power 150 LEDs that are also placed in the sealed box. We put this STVE-TENG box into the water tank. Driven by the wave generated by manually shaking the tank, the 150 LEDs could be lightened (shown in Figure 4d; Video S6, Supporting Information). This is very meaningful because the sea wave energy harvesting based on TENG has been widely used in many fields such as forecasting in marine meteorology[35] and wireless ocean navigation.[36]

In addition, according to the cathodic protection effect, this device can also be used as a power source for protecting metals from corrosion.[37,38] **Figure 5**a shows the illustration of the self-powered electrochemical cathodic protection system. It can be seen that, the positive pole of the rectifier is connected to the Pt electrode, and the negative pole is connected to the carbon steel. Therefore, the electrons generated by the STVE-TENG would be poured onto the carbon steel surface to limit corrosion. The microscopy images in Figure 5b,c are used to observe the efficiency of cathodic protection, and the carbon steels after being polished were immersed into 3.5 wt.% NaCl solution from 0 to 6 h. The results show that the carbon steel surface is completely covered by red rust after being soaked for 2 h, and the degree of corrosion becomes worse with the increase of soaking time. However, there is

Figure 4. The application of the STVE-TENGs. a) 24 LEDs are powered by a STVE-TENG as wearable energy supply devices. b) Demonstration of the STVE-TENG for harvesting the mechanical energy of rotating bicycle wheels. c) Demonstration of lighting 150 LEDs through 3 working STVE-TENGs. d) The power package composed of 15 STVE-TENG was used to recover wave energy and lit 150 LEDs.

only a minor traces of corrosion after being soaked for 6 h with STVE-TENG. Therefore, the cathodic protection system with STVE-TENG is an effective way of electrochemical corrosion protection, which has great application potential in self-powered anticorrosion protection of ships.

3. Conclusion

In summary, we demonstrated a tube-based TENG whose performance is greatly improved by introducing an end electrode and alkali solution. The introduction of the end electrode can successful bring in volume effect. While, alkaline solution can increase the number of negative charges on the surface of PTFE. Both of them are conducive to the improvement of the output performance. In addition, the STVE-TENG also shows sensitivities to salt solution concentration and pH value, which endow it application potential as a biochemical sensor. Furthermore, the device is demonstrated to have wide application possibilities in the field of wearable kinetic energy collection, wave energy collection and electrochemical cathodic protection system.

4. Experimental Section

Reagents and Materials: Transparent polytetrafluoroethylene (PTFE) tube (Inner diameter 16 mm, outer diameter 18 mm) was bought from Taizhou Shunkuo Company, China. Conductive Cu wire with a diameter of 0.4 mm were purchased from Qinghe shenghang metal material Company, China. Conductive Cu tapes with a thickness of 60 µm were purchased from Shenzhen Mileqi Company, China. All the chemical reagents used in this experiment were from Sinopharm Chemical Reagents Company, and the chemicals were analytical pure and can be used directly.

Preparation of Single Electrode Tube-Based TENG and STVE-TENG: PTFE tubes with inner diameter 1.6 cm and outer diameter 1.8 cm were truncated into 10 cm sections. One conducting Cu tape (60 µm thick) with a tunable width L (L = 1, 2, 3, 4, and 5 cm) was bonded to the outer wall of PTFE tube as the external electrode. The two ends of the tube were sealed by PTFE covers. For the STVE-TENG, the Cu wire with diameter of 0.5 mm was arranged at the bottom of one cover and led out through a small hole as the end electrode. Different kinds of solutions (5 mL) were then filled into the PTFE tubes. Both ends were sealed with sealing film to finish the device fabrication.

Characterization: The output currents and voltages were performed by a low-noise current preamplifier (SR570, Stanford Research Systems, Inc., Sunnyvale, CA, USA) and a digital phosphor oscilloscope (DPO 3052, Tektronix, Inc., Beaverton, OR, USA). The charge density from

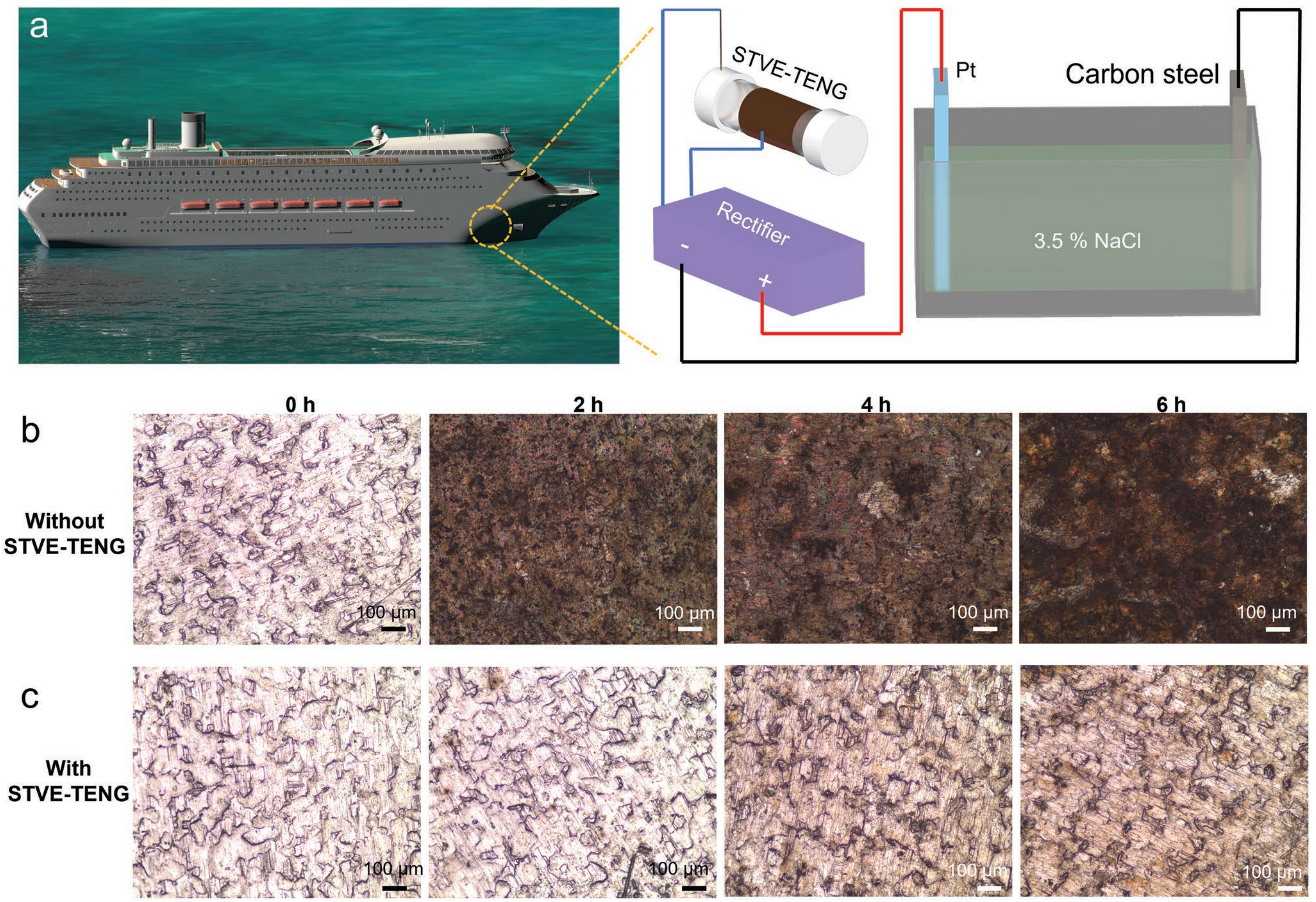

Figure 5. Self-powered electrochemical cathodic protection system based on STVE-TENGs. a) Schematic diagram of Q235 carbon steel cathodic protection experiment setting in 3.5 wt.% NaCl solution. Microscopy images of the Q235 carbon steel immersed in 3.5 wt.% NaCl solution for 0,2,4, and 6 h, separately, connected b) without and c) with STVE-TENGs.

the output signals was measured using an electrometer (Keithley 6514, Cleveland, OH, USA).Informed signed consent was obtained from the volunteer for harvesting the mechanical energy of human motion.

Supporting Information

Supporting Information is available from the Wiley Online Library or from the author.

Acknowledgements

Q.Z. and B.W. contributed equally to this work. This work was supported by the National Natural Science Foundation of China (22004112, 22090050, 21874121, 51902296, 52125205, U20A20166, 61805015 and 61804011), the National Key R & D Program of China (2021YFA1200403, 2018YFE0206900), the Joint NSFC-ISF Research Grant Program (Grant No: 22161142020), the Hubei Provincial Natural Science Foundation of China (2020CFA037), Zhejiang Provincial Natural Science Foundation of China under Grant No. LD21B050001.

Conflict of Interest

The authors declare no conflict of interest.

Data Availability Statement

The data that support the findings of this study are available from the corresponding author upon reasonable request.

Keywords

liquid–solid interfaces, pH value, salt concentration, triboelectric nanogenerators, volume effect

Received: August 7, 2022
Published online: September 14, 2022

[1] L. Yin, K. N. Kim, J. Lv, F. Tehrani, M. Lin, Z. Lin, J. M. Moon, J.-M. Ma, J. Yu, S. Xu, J. Wang, *Nat. Commun.* **2021**, *12*, 1542.
[2] J.-S. Kim, J. Kim, J.-N. Kim, J. Ahn, J.-H. Jeong, I. Park, D. Kim, I.-K. Oh, *Adv. Energy Mater.* **2022**, *12*, 2103076.
[3] Y. Wang, X. Liu, Y. Wang, H. Wang, H. Wang, S. L. Zhang, T. Zhao, M. Y. Xu, Z. L. Wang, *ACS Nano* **2021**, *15*, 15700.
[4] X. Li, J. Luo, K. Han, X. Shi, Z. Ren, Y. Xi, Y. Ying, J. F. Ping, Z. L. Wang, *Nat. Food* **2022**, *3*, 142.
[5] P. Cheng, H. Guo, Z. Wen, C. Zhang, X. Yin, X. Li, D. Liu, W. Song, X. Sun, J. Wang, Z. L. Wang, *Nano Energy* **2019**, *57*, 432.

[6] Z. Lin, B. Zhang, Y. Xie, Z. Wu, J. Yang, Z. L. Wang, *Adv. Funct. Mater.* **2021**, *31*, 2105237.
[7] L. Lin, S. Wang, S. Niu, C. Liu, Y. Xie, Z. L. Wang, *ACS Appl. Mater. Interfaces* **2014**, *6*, 3031.
[8] K. Wang, J. Li, J. Li, C. Wu, S. Yi, Y. Liu, J. Luo, *Nano Energy* **2021**, *87*, 106198.
[9] Q. Zhou, K. Lee, K.-N. Kim, J. G. Park, J. Pan, J. Bae, J. M. Baik, T. Kim, *Nano Energy* **2019**, *57*, 903.
[10] Y. Che, B. Xie, J. Long, Y. Kuang, X. Chen, M. Hou, J. Gao, S. Zhou, B. Fan, Y. He, Y.-T. Zhang, C.-P. Wong, Z. Wang, N. Zhao, *Adv. Mater.* **2021**, *33*, 2104290.
[11] W. Xu, H. Zheng, Y. Liu, X. Zhou, C. Zhang, Y. Song, X. Deng, M. Leung, Z. Yang, R.-X. Xu, Z. Wang, X. Zeng, Z. K. Wang, *Nature* **2020**, *578*, 392.
[12] H. Wu, N. Mendel, D. Ende, G. Zhou, F. Mugele, *Phys. Rev. Lett.* **2020**, *125*, 078301.
[13] L. Wang, Y. Song, W. Xu, W. Li, Y. Jin, S. Gao, S. Yang, C. Wu, S. Wang, Z. K. Wang, *Eco. Mat.* **2021**, *3*, c12116.
[14] X. Xu, Y. Wang, P. Liu, W. Xu, L. Wei, Z. Wang, Z. B. Yang, *Nano Energy* **2021**, *90*, 106573.
[15] N. Zhang, H. Gu, H. Zheng, S. Ye, L. Kang, C. Huang, K. Lu, W. Xu, Q. Miao, Z. Wang, J. Zhang, X. F. Zhou, *Nano Energy* **2020**, *73*, 104748.
[16] H. Wu, Z. Wang, Y. L. Zi, *Adv. Energy Mater.* **2021**, *11*, 2100038.
[17] L. Pan, J. Wang, P. Wang, R. Gao, Y.-C. Wang, X. Zhang, J.-J. Zou, Z. L. Wang, *Nano Res.* **2018**, *11*, 4062.
[18] A. Stetten, D. Golovko, S. Weber, H.-J. Butt, *Soft Matter* **2019**, *15*, 8667.
[19] P. Tajana, A. Selmani, L.-R. Patric, H. Frank, K. Nikola, L. Johannes, *Colloids Surf., A* **2012**, *412*, 120.
[20] R. Zimmermann, U. Freudenberg, R. Schweif, D. Kuttner, C. Werner, *Curr. Opin. Colloid Interface Sci*. **2010**, *15*, 196.
[21] H. Wu, N. Mendel, S. Ham, L. Shui, G. Zhou, F. Mugele, *Adv. Mater.* **2020**, *32*, 2001699.
[22] S. Lin, X. Chen, Z. L. Wang, *Nano Energy* **2020**, *76*, 105070.
[23] S. Lin, L. Xu, A.-C. Wang, Z. L. Wang, *Nat. Commun.* **2020**, *11*, 399.
[24] L. Zhang, X. Li, Y. Zhang, Y. Feng, F. Zhou, D. A. Wang, *Nano Energy* **2020**, *78*, 105370.
[25] Q. Zhou, J. Pan, S. Deng, F. Xia, T. Kim, *Adv. Mater.* **2021**, *33*, 2008276.
[26] Q. Zhou, K. Lee, S. Deng, S. Seo, F. Xia, T. Kim, *Nano Energy* **2021**, *85*, 105980.
[27] T. Jiang, H. Pang, J. An, P. Lu, Y. Feng, X. Liang, W. Zhong, Z. L. Wang, *Adv. Energy Mater.* **2020**, *10*, 2000064.
[28] M. Xu, P. Wang, Y.-C. Wang, S. Zhang, A. Wang, C. Zhang, Z. Wang, X. Pan, Z. L. Wang, *Adv. Energy Mater.* **2018**, *8*, 1702432.
[29] W. Zhong, L. Xu, H. Wang, D. Li, Z. L. Wang, *Nano Energy* **2019**, *66*, 104108.
[30] C. Zhang, L. Zhou, P. Cheng, D. Liu, C. Zhang, X. Li, S. Li, J. Wang, Z. L. Wang, *Adv. Energy Mater.* **2021**, *11*, 2003616.
[31] C. Zhang, W. Yuan, B. Zhang, O. Yang, Y. Liu, L. He, J. Wang, Z. L. Wang, *Adv. Funct. Mater.* **2022**, *32*, 2111775.
[32] C. Zhang, Z. Zhao, O. Yang, W. Yuan, L. Zhou, X. Yin, L. Liu, Y. Li, Z. L. Wang, J. Wang, *Adv. Mater. Technol*. **2020**, *5*, 2000531.
[33] Q. Ma, Y. Li, R. Wang, H. Xu, Q. Du, P. Gao, F. Xia, *Nat. Commun.* **2021**, *12*, 1573.
[34] P. Gao, Q. Ma, D. Ding, D. Wang, X. Lou, T. Zhai, F. Xia, *Nat. Commun.* **2018**, *9*, 4557.
[35] Y. Yang, J. Wen, F. Chen, Y. Hao, X. Gao, T. Jiang, B. Chen, Z. L. Wang, *Adv. Funct. Mater.* **2022**, *32*, 2200521.
[36] Z. Ren, X. Liang, D. Liu, X. Li, J. Ping, Z. Wang, Z. L. Wang, *Adv. Energy Mater.* **2021**, *11*, 2101116.
[37] H. Yang, M. Deng, Q. Zeng, X. Zhang, J. Hu, Q. Tang, H. Yang, C. Hu, Y. Xi, Z. L. Wang, *ACS Nano* **2020**, *14*, 3328.
[38] C. Zhang, B. Zhang, W. Yuan, O. Yang, Y. Liu, L. He, Z. Zhao, L. Zhou, J. Wang, Z. L. Wang, *ACS Appl. Mater. Interfaces* **2022**, *14*, 8605.